ACS Partner Journal

ACCOUNTS of materials research

pubs.acs.org/amrcda

Article

Gas Separation Membranes with Atom-Thick Nanopores: The Potential of Nanoporous Single-Layer Graphene

Luis Francisco Villalobos,[#] Deepu J. Babu,[#] Kuang-Jung Hsu,[#] Cédric Van Goethem,[#] and Kumar Varoon Agrawal*

Cite This: *Acc. Mater. Res.* 2022, 3, 1073–1087

Read Online

ACCESS | Metrics & More | Article Recommendations

CONSPECTUS: Gas separation is one of the most important industrial processes and is poised to take a larger role in the transition to renewable energy, e.g., carbon capture and hydrogen purification. Conventional gas separation processes involving cryogenic distillation, solvents, and sorbents are energy intensive, and as a result, the energy footprint of gas separations in the chemical industry is extraordinarily high. This has motivated fundamental research toward the development of novel materials for high-performance membranes to improve the energy efficiency of gas separation. These novel materials are expected to overcome the intrinsic limitations of the conventional membrane material, i.e., polymers, where a longstanding trade-off between the separation selectivity and the permeance has motivated research into nanoporous materials as the selective layer for the membranes. In this context, atom-thick materials such as nanoporous single-layer graphene constitute the ultimate limit for the selective layer. Gas transport from atom-thick nanopores is extremely fast, dependent primarily on the energy barrier that the gas molecule experiences in translocating the nanopore. Consequently, the difference in the energy barriers for two gas molecules determines the gas pair selectivity.

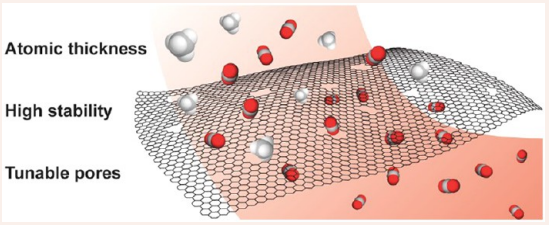

In this Account, we summarize the development in the field of nanoporous single-layer graphene membranes for gas separation. We start by discussing the mechanism for gas transport across atom-thick nanopores, which then yields the crucial design elements needed to achieve high-performance membranes: (i) nanopores with an adequate electron-density gap to sieve the desired gas component (e.g., smaller than 0.289, 0.33, 0.346, 0.362, and 0.38 nm for H_2, CO_2, O_2, N_2, and CH_4, respectively), (ii) narrow pore size distribution to limit the nonselective effusive transport from the tail end of the distribution, and (iii) high density of selective pores. We discuss and compare the state-of-the-art bottom-up and top-down routes for the synthesis of nanoporous graphene films. Mechanistic insights and parameters controlling the size, distribution, and density of nanopores are discussed. Fundamental insights are provided into the reaction of ozone with graphene, which has been successfully used by our group to develop membranes with record-high carbon capture performance. Postsynthetic modifications, which allow the tuning of the transport by (i) tailoring the relative contributions of adsorbed-phase and gas-phase transport, (ii) competitive adsorption, and (iii) molecular cutoff adjustment, are discussed. Finally, we discuss practical aspects that are crucial in successfully preparing practical membranes using atom-thick materials as the selective layer, allowing the eventual scale-up of these membranes. Crack- and tear-free preparation of membranes is discussed using the approach of mechanical reinforcement of graphene with nanoporous carbon and polymers, which led to the first reports of millimeter- and centimeter-scale gas-sieving membranes in the year 2018 and 2021, respectively. We conclude with insights and perspectives highlighting the key scientific and technological gaps that must be addressed in the future research.

■ INTRODUCTION

The conventional gas separation processes are energy intensive because they rely on thermal energy. Membrane-based gas separation is attractive because it does not rely on thermal energy for separation. It is environment-friendly as no waste is produced. Nanoporous two-dimensional (2D) films when applied as the selective layer of the membrane can overcome several limitations of the conventional polymeric membranes. Nanoporous 2D films are especially attractive for breaking the intrinsic performance trade-off[1,2] of the polymeric materials. In addition, they help realize chemically and thermally robust membranes that do not have issues such as aging and plasticization. Several chemically and thermally robust 2D materials, e.g., single-layer graphene (SLG), hexagonal boron nitride, transition metal dichalcogenides, graphitic carbon nitride, graphynes, etc. (Figure 1A) are attractive for this purpose. Atom-thick nanopores can be incorporated into these

Received: July 20, 2022
Revised: August 30, 2022
Published: September 13, 2022

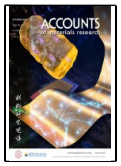

ACS Publications

© 2022 The Authors. Co-published by ShanghaiTech University and American Chemical Society

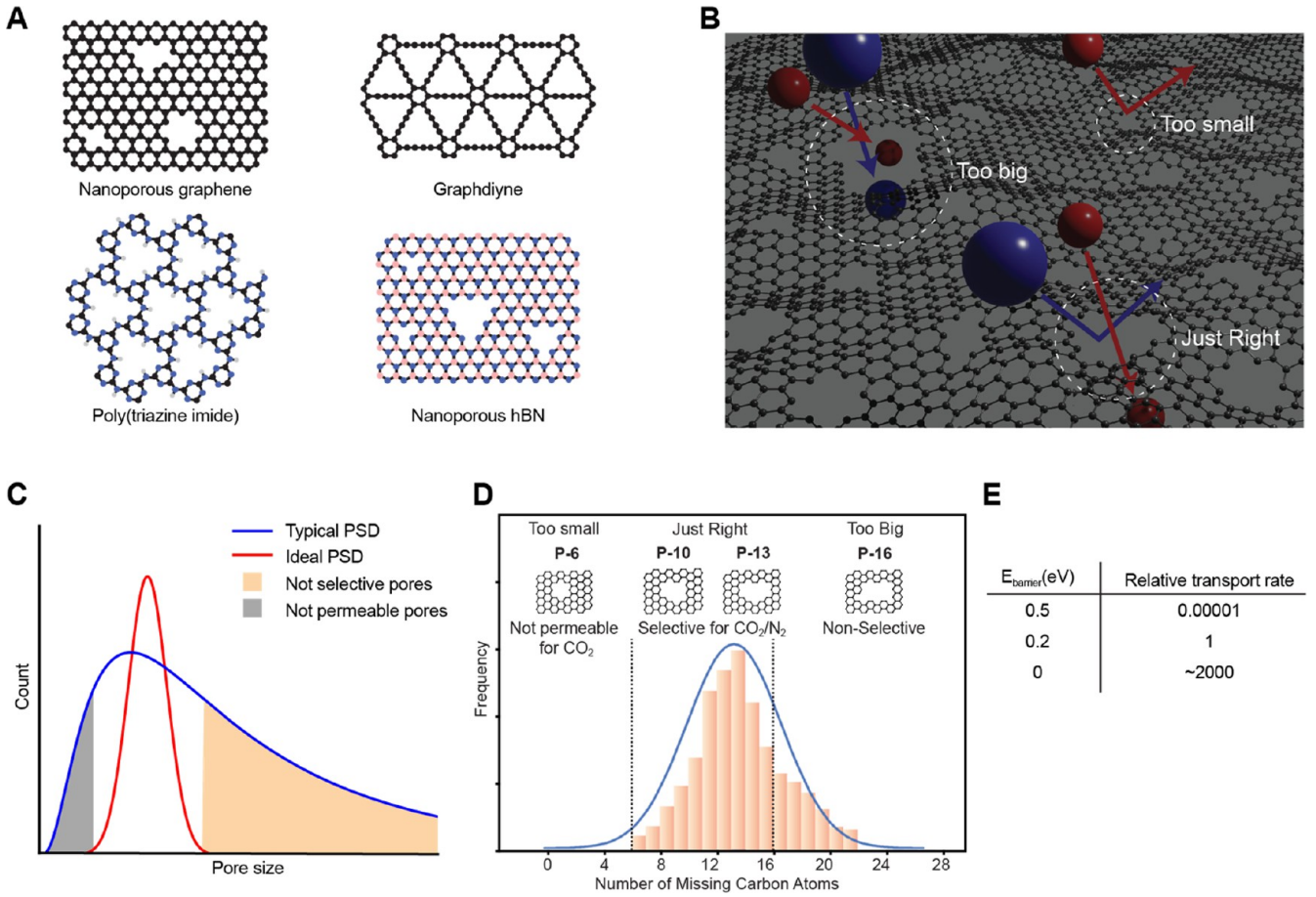

Figure 1. Atom-thick nanopores for gas sieving. (A) Examples of 2D materials with atom-thick nanopores suitable for gas separations. (B) Schematic of N-SLG showing the three general kinds of pores for a given separation. (C) Lognormal PSD that is typically produced in N-SLG by etching techniques. (D) Example of a PSD for CO_2/N_2 separation consisting of pores with 1−28 missing carbon atoms. Smaller pores do not contribute to permeation (large energy barrier), and pores larger than 16 missing carbon atoms are not selective (no energy barrier). (E) Energy barrier for gas transport through graphene nanopores and its corresponding relative transport rate.

materials as vacancy defects. Nanopores in SLG constitute the thinnest possible permselective layer.[3,4] Single-atom thickness of the nanopore translates into extremely small molecular diffusion path length and consequently high permeance.[5] Molecular-sized nanopores differentiate gas molecules based on the relative size difference of gas molecules with respect to the nanopores, a concept termed molecular sieving.

Nanoporous SLG (N-SLG) has been widely studied for gas separation given the high chemical, thermal, and mechanical robustness of graphene. Experimental studies have shown that porous graphene suspended over a submicron-sized support pore can sustain transmembrane pressure up to several bars.[6,7] Unique for an inorganic material, graphene is flexible attributing to its 2D lattice. Large-scale roll-to-roll synthesis of graphene have been already demonstrated for application in electronics.[8,9]

The first theoretical paper on gas transport from graphene nanopore was reported by Jiang et al. in the year 2009, which discussed the tremendous potential of graphene for gas separation based on molecular sieving.[10] They showed that a pore-10, where 10 indicates the number of missing carbon atoms in the pore, can sieve H_2 from CH_4 with an exponential selectivity (10^8−10^{23} depending on the edge functional groups). Subsequent theoretical studies have predicted that high gas permeance is expected, on the order of 10^4−10^5 gas permeation units or GPU where 1 GPU = 3.35×10^{-10} mol m^{-2} s^{-1} Pa^{-1}, if a high density of nanopores can be incorporated in the lattice ($\sim 10^{13}$ cm^{-2}).[11] Gas adsorption plays a significant role when the molecule of interest has a strong affinity with graphene lattice or functional group along the pore edge. Therefore, pore functionalization can be used to manipulate the transport properties of gas molecules.[12]

A proof-of-concept experiment for gas sieving from graphene nanopore was demonstrated in the year 2012 by Bunch and co-workers. They measured the deflation rate of a pressurized graphene microballoon to estimate the gas flux. Pores were incorporated by oxidation of graphene with UV/O_3.[13] Further advances in this field faced a stiff challenge from preparing larger area membranes in a crack-free manner. It was not until the year 2018 that the size-sieving behavior was demonstrated from nanopores in SLG by directly measuring the composition of mixed gases crossing the nanopores. Briefly, crack- and tear-free films, large enough (1 mm^2) for performing gas mixture separation studies, were suspended on a macroporous support.[14] This was achieved by depositing a nanoporous carbon (NPC) film on top of graphene as a mechanical reinforcement layer, which prevented crack formation during graphene transfer from the CVD substrate.[14,15] The crack-free transfer protocol ignited experimental advancements in gas separation and has allowed the development of uniform and

https://doi.org/10.1021/accountsmr.2c00143
Acc. Mater. Res. 2022, 3, 1073−1087

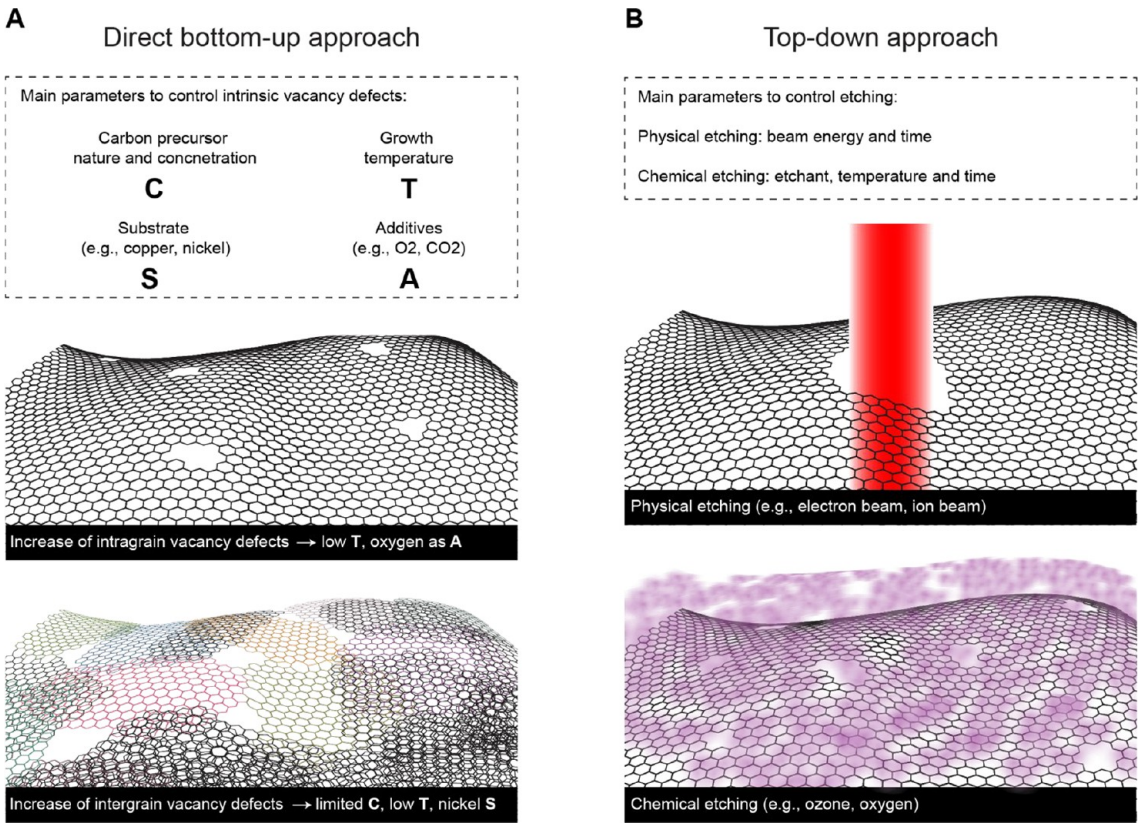

Figure 2. Engineering gas-sieving pores by bottom-up and top-down approaches. (A) Intrinsic vacancy defects typically found in CVD graphene (top), bottom-up approaches to maximize the intragrain vacancy defects (middle), and intergrain vacancy defects (bottom). (B) Pristine graphene lattice (top) and the postsynthetic etching routes to incorporate vacancy defects: physical etching (middle) and chemical etching (bottom).

scalable chemical etching approaches.[14,16−20] However, challenges still linger ahead especially related to advancing the gas separation performance and to the scalable fabrication of large-area membranes.

In this Account, we summarize recent developments in this field focusing on the approaches for the incorporation of vacancy defects, a toolbox for modulating gas transport, characterization of nanopores, and finally practical aspects that are crucial in scaling up membranes. We conclude this Account with a perspective highlighting the key scientific and technological gaps, which must be addressed in the future.

GAS SIEVING FROM GRAPHENE NANOPORES

Achieving gas sieving from N-SLG membranes requires four key design elements:

(i) Å-scale pores to sieve gases based on their relative size with respect to the nanopore (Figure 1B). The gas flux is directly proportional to the energy barrier that a molecule experiences at the transition state while crossing the pore. Therefore, to realize size sieving, the pore size should be commensurate to the molecule of interest.

(ii) A narrow pore size distribution (PSD). It is currently not possible to incorporate monomodal pores in graphene, and typically a log-normal PSD is observed by the state-of-the-art pore incorporation techniques (Figure 1C). Molecules do not experience an energy barrier while crossing larger nanopores at the tail end of the distribution (Figure 1D,E). As a result, these pores yield large permeance and poor selectivity.

(iii) A high density (10^{12}−10^{13} cm^{-2}) of gas selective nanopores to maximize gas permeance.

(iv) Adequate surface and edge functional groups to favor interactions with the targeted molecules.

Pores can be incorporated into graphene either by postsynthetic lattice etching (top-down route) or by direct crystallization of nanoporous graphene lattice (bottom-up route). Postsynthetic etching of the graphene lattice is promising for achieving a fine control over PSD. Direct crystallization of porous graphene is attractive to improve the scalability of graphene membranes. In this section, we review advances in this area (Figure 2).

Postsynthetic etching can be achieved by (i) physical etching involving knocking out carbon atoms by energetic electron[21] or ion[22] beams (Figure 3A−C) and (ii) oxidative chemistry involving gasification of carbon atoms into CO/CO_2 using O_2,[23] O_2 plasma,[24,25] O_3,[14,17,26] and UV/O_3[13] (Figure 3D−G). We note that the incorporation of a high density of gas-sieving nanopores is challenging because often reaction conditions that generate new pores (nucleation event) also expand the existing pores; i.e., the pore nucleation and expansion steps are coupled. So while pore density can be increased by a prolonged etching, it also generates a broader PSD. Therefore, decoupling pore nucleation and expansion is an extremely attractive research goal.

Physical etching can be used to precisely control the position of the nanopore by selecting the location for knocking out carbon atom using energetic beams. Recent advances have shown the incorporation of pores in the size range of a few nanometers.[22] However, this route is challenging to incorpo-

https://doi.org/10.1021/accountsmr.2c00143
Acc. Mater. Res. 2022, 3, 1073−1087

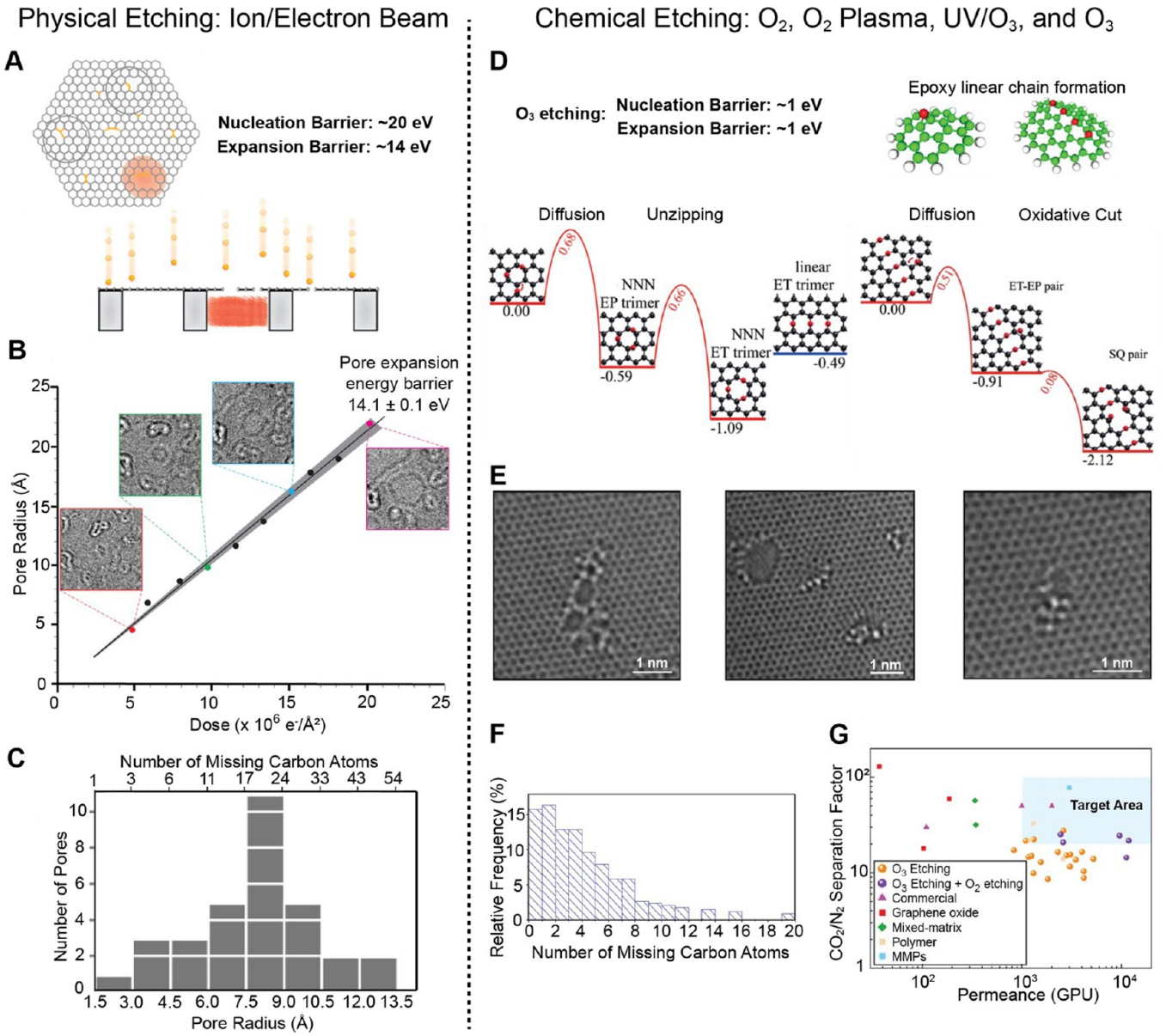

Figure 3. Postsynthetic etching. (A) Illustration of physical etching, such as the ion/electron beam, on graphene lattice with corresponding nucleation and expansion energy barriers. Reprinted with permission from ref 29. Copyright 2017 American Chemical Society. (B) Energy barrier of pore expansion extracted from the trajectory of graphene pore growth with increasing electron dose. (C) Pore size distribution of nanopores etched by electron beams in TEM. Panels B and C reprinted with permission from ref 28. Copyright 2012 National Academy of Sciences. (D) Evolution of defects in graphene by oxidation: epoxy and ether groups cluster and finally lead to C−C bond breakage (energy is in eV unit). Reprinted with permission from refs 30 and 31. Copyright 2006 The American Physical Society and 2012 American Chemical Society. (E) High-resolution transmission electron microscopy (HRTEM) images of nanopores in graphene lattice after O_3 etching treatment (2 min at 80 °C). Reprinted with permission from ref 14. Copyright 2018 The Authors. (F) Narrow PSD of nanoporous graphene after O_3 etching treatment. (G) Carbon capture performance of nanoporous graphene etched by O_3 and O_2 compared to that from the state-of-the-art membranes. Panels F and G reprinted with permission from ref 20. Copyright 2021 American Association for the Advancement of Science.

rate Å-scale pores needed for gas sieving because the energy barrier for knocking out a carbon atom from graphene's basal plane is much higher (~20−21 eV) compared to that needed from an edge (~14 eV,[27,28] Figure 3B). As a result, the rate of pore expansion is much faster than the rate of nucleation (Figure 3C).

Chemical etching is highly promising because it can be carried out uniformly over a large area of graphene in a scalable way. It provides an opportunity to control the pore size at the Å scale by controlling the chemical transformation of the lattice at the atomic level. Chemical etching can be described by the following general steps:[32,33] (i) chemisorption of the etchant forming oxidative groups such as epoxies, (ii) evolution of epoxy groups into energy minimizing clusters, and (iii) gasification of carbon atoms from the cluster leading to the formation of a vacancy defect. In this case, the energy barriers for pore nucleation and expansion are similar (O(1 eV)).

We have recently shown that O_3 gas can chemisorb on graphene even at room temperature, making O_3 a user-friendly and scalable gaseous etchant.[14] Etching starts with the formation of an epoxy group. The energy barrier for

https://doi.org/10.1021/accountsmr.2c00143
Acc. Mater. Res. 2022, 3, 1073−1087

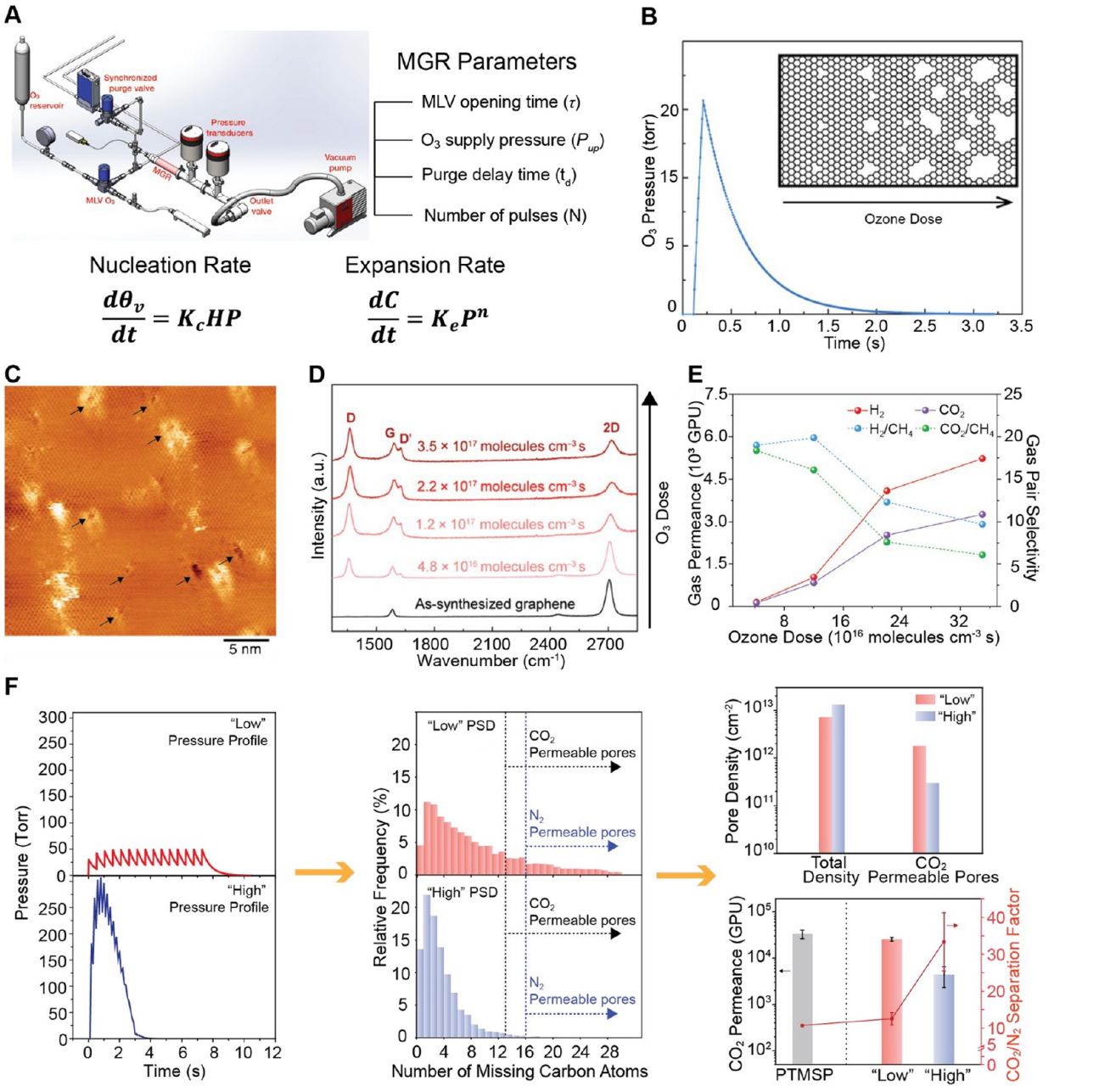

Figure 4. Millisecond O_3 etching. (A) Schematic of O_3 millisecond gasification reactor (MGR) with its control parameters for nucleation and expansion rate as a function of pressure. (B) Pressure profile of the O_3 pulse in the MGR chamber. (C) STM images of highly oriented pyrolytic graphite (HOPG) oxidized by MGR at 250 °C. (D) Raman spectrum showing the evolution of the N-SLG with increasing O_3 dose. (E) Evolution of the gas permeance and gas pair selectivities as a function of the O_3 dosage. Panels A–E reprinted with permission from ref 20. Copyright 2021 The Authors. (F) Narrower PSD by multipulse O_3 etching resulting in an improved separation performance. Reprinted with permission from ref 18. Copyright 2021 The Authors.

chemisorption of O_3 into epoxy has been predicted by ab initio calculations to be 0.75 eV.[32] We recently estimated an energy barrier of 0.67 eV based on counting the concentration of oxygen functional groups on a graphitic lattice as a function of O_3 exposure conditions using X-ray photoelectron spectroscopy (XPS).[20] The epoxy groups have been reported to form cyclic trimers and finally cluster as a honeycomb network of cyclic trimers to minimize the net energy of epoxy/graphene system (Figure 3D).[34] Subsequently, a significant strain present in the cluster leads to the cleavage of C–O–C bond, leading to the formation of a pair of semiquinone groups.[31,35] This is followed by gasification of the edge atoms as CO/CO_2.[33] Understanding and controlling the formation of clusters and subsequent transformation into vacancy defects is key to controlling the PSD in graphene.

Recently, we showed that CO_2-sieving pores can be incorporated into graphene by etching in a millisecond time scale (Figure 4A–C).[19,20] A short millisecond reaction limits pore expansion while a high oxidation temperature (250–300 °C) promotes chemisorption increasing the pore density. By varying the O_3 exposure, we could prepare membranes with attractive gas separation performance (Figure 4D,E). Recently, by using multiple pulses of O_3 in a short time, we were able to increase pore density resulting in improved CO_2-sieving (CO_2

https://doi.org/10.1021/accountsmr.2c00143
Acc. Mater. Res. 2022, 3, 1073–1087

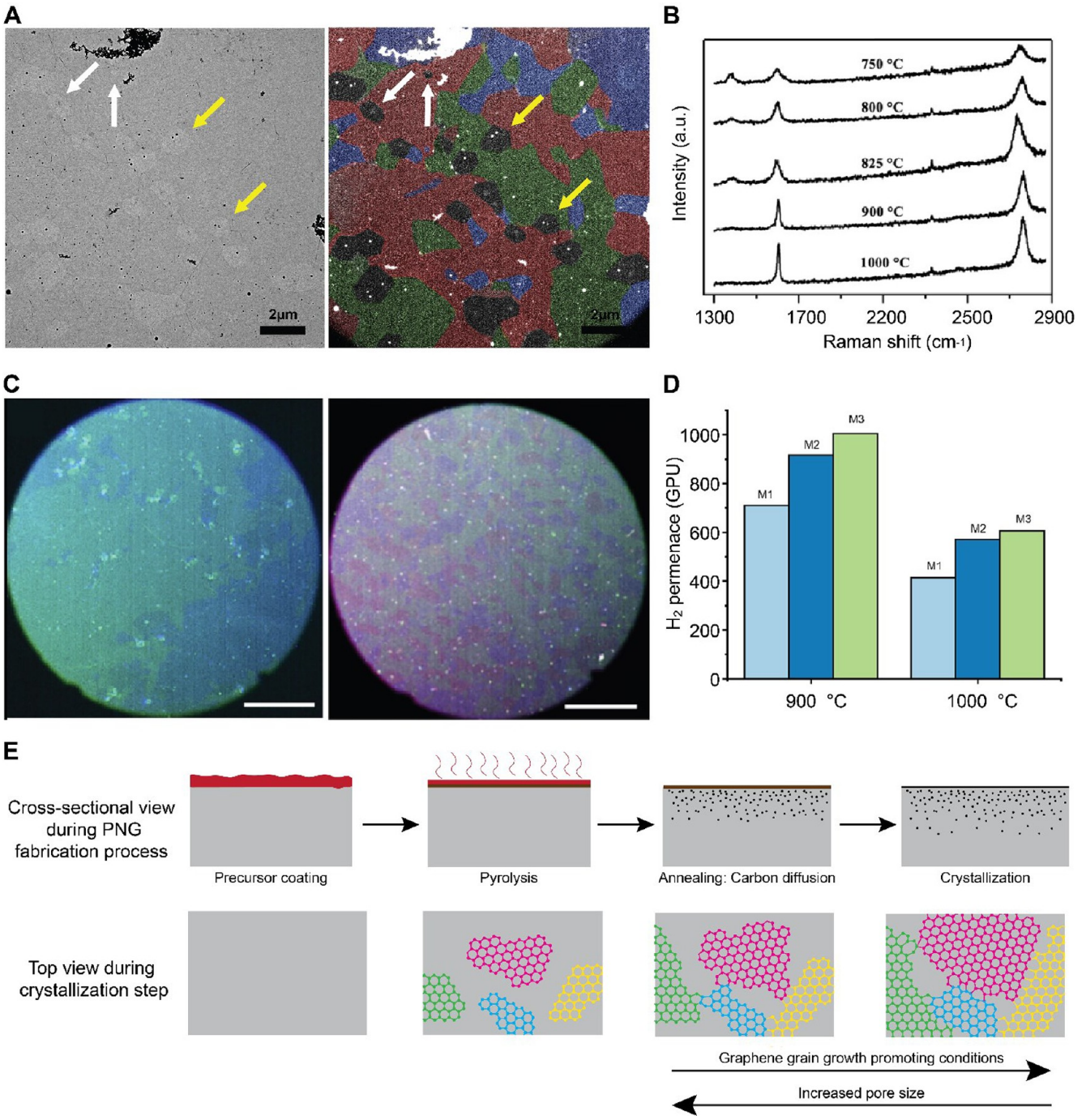

Figure 5. Bottom-up synthesis of N-SLG. (A) Bright-field (left) and false-colored dark-field (DF, right) transmission electron microscope (TEM) images of CVD graphene etched with CO_2 to reveal intragrain and intergrain intrinsic defects. Reprinted with permission from ref 36. Copyright 2022 The Authors. (B) Raman spectroscopy of benzene-derived graphene synthesized at various temperatures. Reprinted with permission from ref 38. Copyright 2019 The Authors. (C) False-colored DF-TEM images of benzene-derived graphene synthesized at 1000 (left) and 825 °C (right). Reprinted with permission from ref 38. Copyright 2019 The Authors. (D) H_2 permeance at 30 °C of benzene-derived graphene synthesized at 900 and 1000 °C. Adapted with permission from ref 38. Copyright The Authors. (E) Schematic illustration of the PNG synthesis process and pore formation in PNG.

permeance of 4400 GPU and CO_2/N_2 selectivity of 33.4, Figure 4F).[18] Briefly, pore nucleation was promoted by a higher O_3 pressure in multipulse exposure. This is because chemisorption, and therefore, nucleation is proportional to the O_3 pressure, P. However, pore expansion is proportional to P^n, where n is less than 1 because an O_3 molecule can yield more than one functional group at the pore edge. As a result, a higher O_3 dose in a short time leads to a narrower PSD (Figure 4F).

The direct bottom-up synthesis is highly attractive for scalable production of nanoporous graphene. The presence of porosity in graphene in the form of intrinsic vacancy defects has been known for some time now. Intrinsic defects in graphene are both grain-boundary defects (arising from imperfect grain stitching) and intragrain defects (formed by

https://doi.org/10.1021/accountsmr.2c00143
Acc. Mater. Res. 2022, 3, 1073−1087

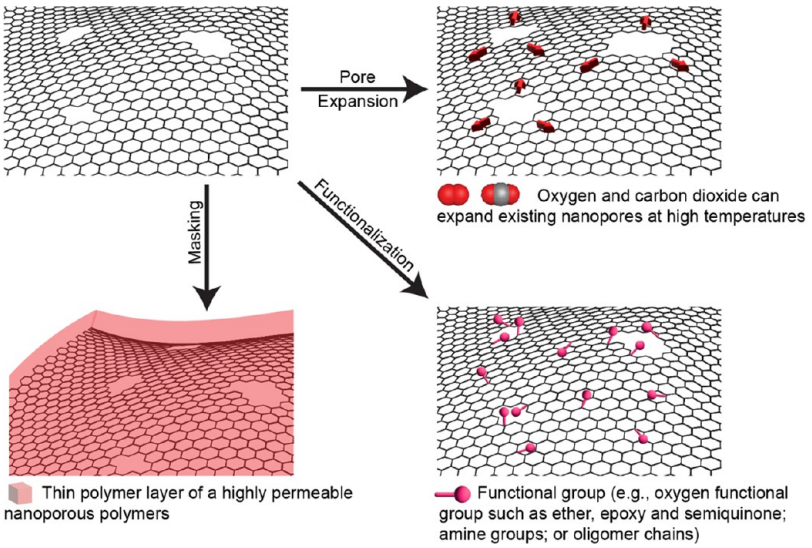

Figure 6. Toolbox to tune graphene nanopores for high-performance gas separations.

lattice etching in the presence of leaking O_2 in the CVD reactor). We recently visualized these two kinds of defects by expanding them with CO_2 at 800 °C.[36] We could identify several grain-boundary defects as well as intragrain defects although the density of the former was significantly higher (Figure 5A). The relative population of these defects is sensitive to the CVD conditions, including the leak rate of the CVD reactor.

Intrinsic vacancy defects can be regulated by varying growth temperature, carbon precursor, and the catalytic substrate. CVD temperature affects graphene grain growth, its morphology, and the resulting "quality" and, hence, the defect density. Kidambi et al. reported an increased defect density upon lowering CVD temperature from 1000 to 900 °C.[37] We recently reported benzene-derived SLG where the average graphene grain size reduces from 20 to 1 μm by reducing the CVD temperature from 1000 to 825 °C (Figure 5B,C).[38] This was also reflected in increased H_2 permeance (600 to 1000 GPU, Figure 5D).[38] The carbon precursor controls the grain morphology because it controls the nature and the concentration of active growth species. A favorable dehydrogenation kinetics of an unsaturated molecule (e.g., benzene) promotes growth at a lower temperature. Comparing H_2 transport from intrinsic vacancy defects in graphene synthesized using methane and benzene, one observes a relatively higher H_2 permeance and lower H_2/CH_4 selectivity from the benzene-derived graphene (5−8 and 6−25 for benzene- and methane-derived graphene, respectively).[14,38]

The catalytic CVD substrate catalyzes precursor breakdown into active species and ultimately controls grain morphology.[39] For CVD on copper, the entire sequence of reaction and diffusion of the precursors takes place on the external surface (surface growth mechanism[40]). However, substrates with a significant C solubility (e.g., Ni or Rh) crystallize graphene via the precipitation route.[41] We recently exploited this route to prepare porous graphene with a high density of intrinsic vacancy defects. Depositing a small amount of carbon precursor on the foil as a thin polymer film followed by a short heat treatment at 500 °C, produced porous nanocrystalline graphene (PNG) (Figure 5E).[42] The heat treatment resulted in the pyrolysis of the polymer, which built a C reservoir in the Ni matrix. Upon cooling, the C solubility decreased, which led to a high degree of supersaturation and eventual precipitation of C as graphene grains on the surface of the foil. Because of the intentionally limited C loading, complete intergrowth of the graphene grains forming the PNG film was not achieved. Rather, films with a high density of grain-boundary defects (2.1×10^{12} cm^{-2}; measured from AC-HRTEM images) similar to that obtained by the state-of-the-art postsynthetic etching techniques, were obtained. The type of vacancy defects (nanopores) predominantly found in PNG films are intergrain defects produced by the incomplete stitching of three or more grains (Figure 8H−J).

■ TOOLBOX FOR TAILORING GAS TRANSPORT

The transport of gas molecules through N-SLG can be tailored by postsynthetic modification, by nanopore functionalization, by masking, and by adjusting the PSD (Figure 6).

Nanopore functionalization can reduce the electron-density gap and alter molecular interactions either by modifying the molecular diffusivity or by enhancing molecular affinity to the lattice. The effect of functionalization is best studied using mixtures because competitive interactions often dominate the transport of molecules. Molecular dynamic insights have shown that relatively large nanopores can be converted to CO_2-selective nanopores either by inducing a surface charge[43] or by depositing a film of ionic liquids (IL).[44] Recently, Guo et al. verified experimentally that coating a nonselective N-SLG with a thin layer of IL could produce membranes with CO_2/N_2 selectivities of up to 32.[45]

We showed that a room temperature O_3 treatment can graft O-functional groups at the pore edges, resulting in improved gas-sieving performance.[14] A decreased H_2 permeance accompanied by an increased H_2/CH_4 selectivity (by 1.5-fold). This behavior is consistent with a reduced electron-density gap in the pore after atomic-scale functionalization. The reduction depends on the size of the functional groups grafted at the edge of the nanopores. For example, a semiquinone group would reduce the electron-density gap by 1.2 Å. To enhance adsorption affinity, we grafted N-SLG with polyethylenimine (PEI) chains hosting CO_2-philic groups[46] (Figure 7A). PEI was grafted on the graphene lattice via the ring-opening chemistry of epoxy groups in oxidized graphene

https://doi.org/10.1021/accountsmr.2c00143
Acc. Mater. Res. 2022, 3, 1073−1087

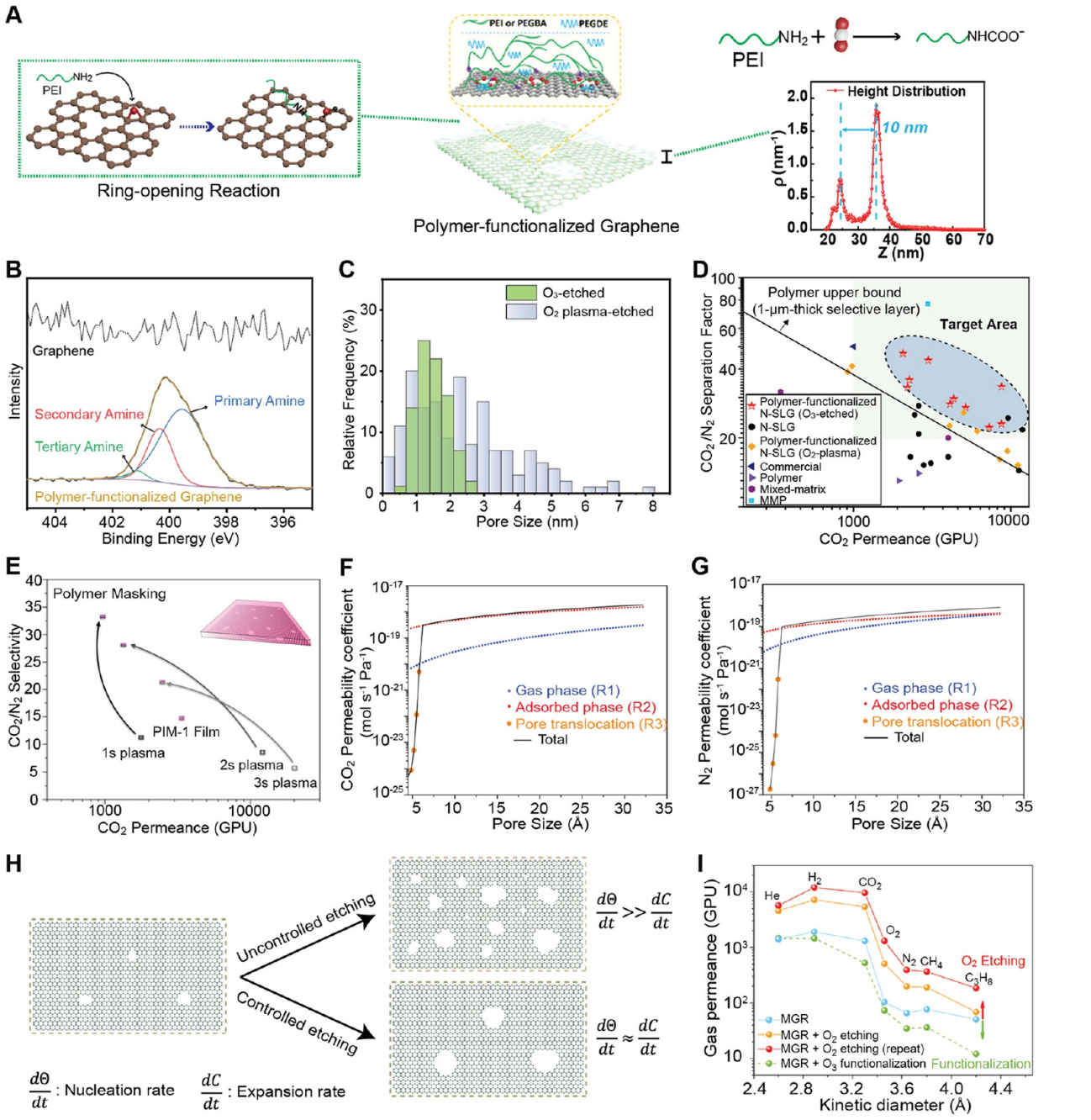

Figure 7. Modification of graphene nanopores. (A) Illustration of polymer-functionalization by the ring-opening reaction leading to a 10 nm thick PEI film. Portions of panel A reprinted with permission from ref 46. Copyright 2019 The Authors. (B) N 1s XPS data confirming functionalization. (C) Comparison between PSD of O_3-etched and O_2 plasma-etched nanopores. (D) Carbon capture performance of polymer-functionalized graphene compared to nanoporous graphene and the state-of-the-art membranes. Panels B–D reprinted with permission from ref 18. Copyright 2021 The Authors. (E) CO_2/N_2 separation performance when graphene is masked by PIM-1. CO_2 (F) and N_2 (G) transport as a function of pore size using different transport pathways. Panels E–G reprinted with permission from ref 48. Copyright 2020 Wiley-VCH. (H) Schematic illustration showing the advantage of controlling nucleation and expansion rates. Reprinted with permission from ref 36. Copyright 2022 The Authors. (I) Effect of O_2 etching on the gas permeance of MGR-based N-SLG. Reprinted with permission from ref 20. Copyright 2021 The Authors.

(Figure 7B). PEI chains were swollen with poly(ethylene glycol)−dimethyl ether to improve gas diffusivity. Ten nanometer thick selective layers prepared by this strategy yielded attractive CO_2/N_2 separation performance (CO_2 permeance of 6180 GPU and CO_2/N_2 separation factor of 22.5). Improving the PSD by controlled O_3 etching followed by PEI functionalization further improved the separation performance (CO_2 permeance of 8730 GPU with CO_2/N_2 separation factor of 33.4, Figure 7C,D).

An advantage of depositing polymeric chains on graphene is that the pores are masked by the chains. As a result, the direct access to the pores from the gas phase is blocked. This helps to reduce the rapid effusion through any large nonselective nanopore. We demonstrated this by depositing a polymer of intrinsic microporosity (PIM-1, Figure 7E).[47] The obstruction of direct gas-phase transport reduced the N_2 transport much more relative to CO_2, thanks to a stronger adsorbed-phase

https://doi.org/10.1021/accountsmr.2c00143
Acc. Mater. Res. 2022, 3, 1073−1087

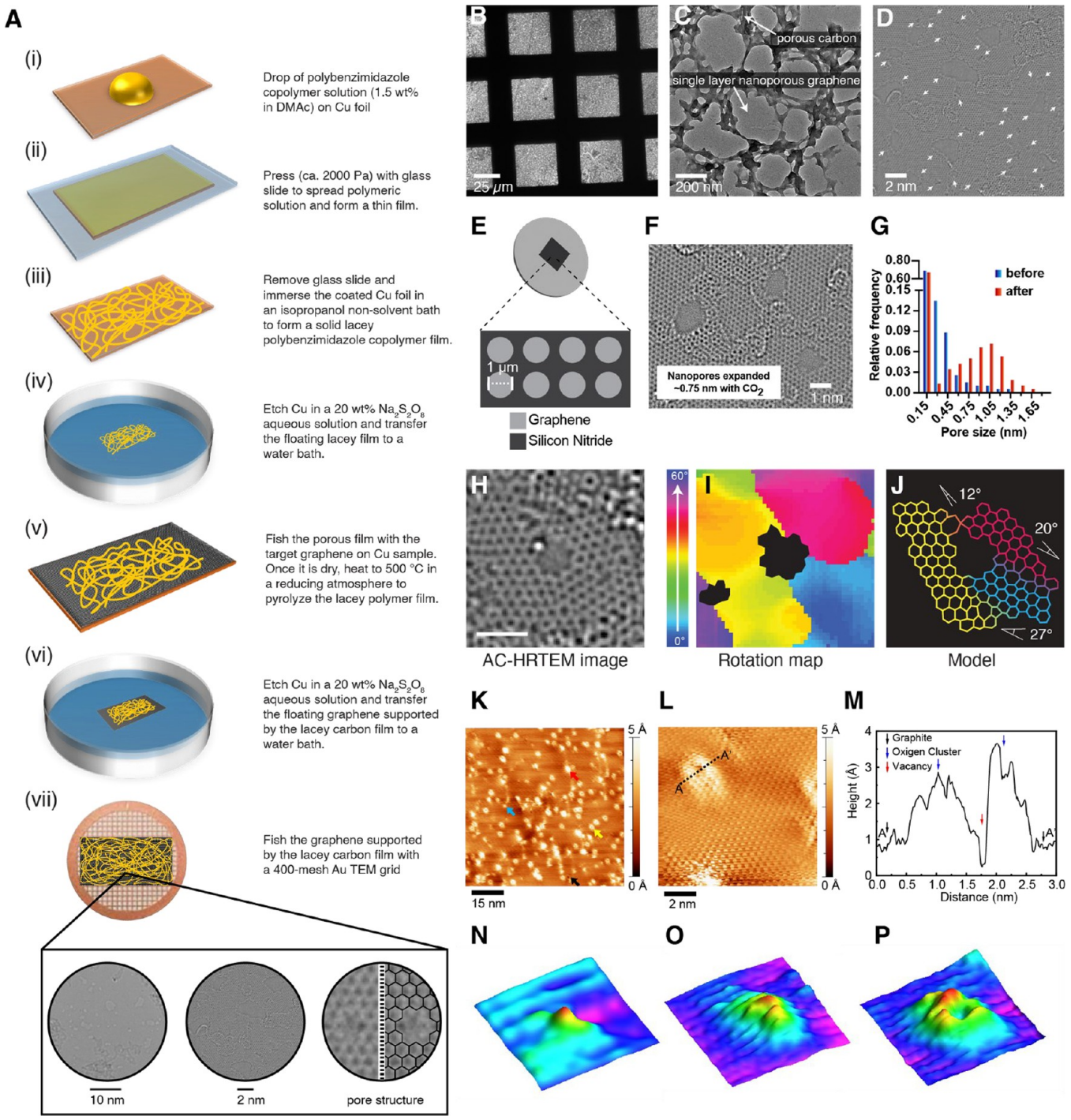

Figure 8. AC-HRTEM and STM analsysis of N-SLG. (A) Contamination-free preparation of N-SLG specimen for AC-HRTEM analysis using lacey carbon film assisted transfer. TEM (B, C) and AC-HRTEM (D) images of nanoporous graphene supported by the lacey carbon film (step vii of panel A). Panels A–D reprinted with permission from ref 51. Copyright 2021 The Authors. (E) CVD graphene suspended on a holey silicon nitride grid. (F) AC-HRTEM image of nanopores obtained by expansion of nanopores by CO_2. (G) Shift in PSD after the CO_2 expansion. Panels F–G reprinted with permission from ref 36. Copyright 2022 The Authors. (H) AC-HRTEM image of a graphene nanopore created by the incomplete stitching of three misaligned nanograins and its orientation map done by an advanced automatic image analysis (I) and a manual fitting (J). Panels H–J reprinted with permission from ref 42. Copyright 2021 National Academy of Sciences. (K and L) STM images of an O_3-treated HOPG (bias voltage, −0.05 V; tunneling current, 0.5 nA). (M) Cross-sectional profile of the line A–A′ drawn in panel L. (N–P) Three-dimensional STM images (5 nm × 5 nm; bias voltage, −0.05 V; tunneling current, 0.5 nA) of an oxidized HOPG surface to illustrate the different etching stages of nanopore formation. (N) Small epoxy clusters and (O) larger clusters where carbon vacancies are not yet formed. (P) Donut-shaped clusters where carbon vacancies form in the middle of the cluster. Panels K–P reprinted with permission from ref 34. Copyright 2022 The Authors.

transport of CO_2 (Figure 7F,G). In general, this route can be applied using several high-permeability polymers.[18]

Controlled pore expansion can be used to manipulate PSD and molecular cutoff. We recently demonstrated this with O_2

https://doi.org/10.1021/accountsmr.2c00143
Acc. Mater. Res. 2022, 3, 1073−1087

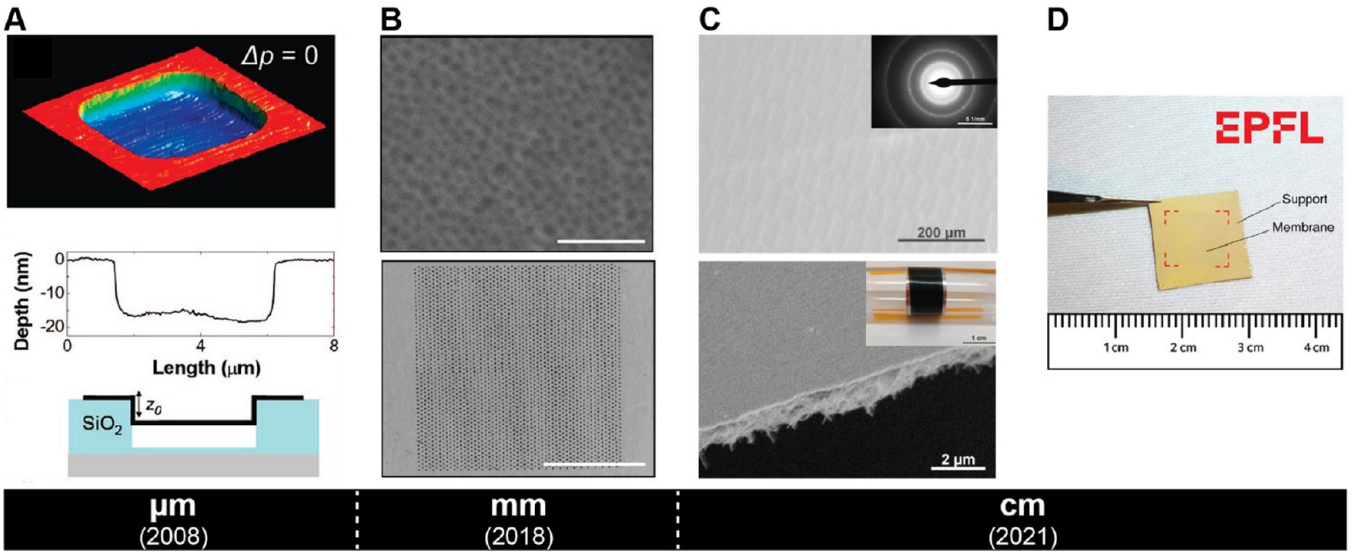

Figure 9. Evolution of the scale-up of NSLG membranes. (A) Initial microballoon experiment with an area of a few μm^2 demonstrated the impermeability of graphene. Reprinted with permission from ref 5. Copyright 2008 American Chemical Society. (B) Scanning electron microscopy (SEM) images of the NPC-supported SLG film. This approach realized millimeter-scale gas-sieving membranes. Scale bars are 200 nm and 0.5 mm in the top and bottom images, respectively. Reprinted with permission from ref 14. Copyright 2018 The Authors. (C) SEM images and photographs of dual carbon film (NPC and MWNT) reinforced N-SLG. Centimeter-scale size-sieving N-SLG was realized. Reprinted with permission from ref 16. Copyright 2021 The Authors. (D) Centimeter-scale demonstration of N-SLG membrane reinforced with a nanoporous polymer supported on metal mesh support. Reprinted with permission from ref 18. Copyright 2021 The Authors.

or low-concentration O_3 (Figure 7H). A controlled expansion of pores was achieved by an in situ exposure to O_2 at 200 °C inside a membrane module (Figure 7I),[20] where a concerted increase in CO_2 permeance and selectivity with N_2 was achieved. A model of pore expansion predicted an expansion rate of 0.14 Å h^{-1} under these conditions, consistent with shifting the molecular cutoff in favor of a rapid permeation of CO_2. This was also evidenced by the fact that O_2/N_2 selectivity increased during this slow expansion in O_2. Recently, we demonstrated that CO_2 can be used as an etchant for existing pores in N-SLG where only pore expansion events take place and new nucleation events are prohibited.[36] This is because nucleation of new defects on the basal plane of graphene requires surpassing a prohibitive energy barrier (5 eV). A controllable etching rate of 0.6 to 280 nm min^{-1} could be achieved by varying the etching temperature between 750 and 1000 °C. This etching strategy is promising for various separations ranging from gas to ions.[36] We note that etching at such high temperatures did not produce cracks when done on Cu-supported graphene, but cracks could develop if the graphene is supported on a porous substrate with a different coefficient of thermal expansion.

UNDERSTANDING THE STRUCTURE OF NANOPORES

Developing a robust understanding of gas transport observed from the N-SLG membranes requires linking nanopore structure with the observed transport properties. However, current understanding is limited because of the lack of understanding of the "real" pore structure, including functional groups around the pores that participate in the gas transport.

The most common characterization for nanopore structure is based on aberration-corrected high-resolution transmission electron microscopy (AC-HRTEM). It is a powerful tool to resolve the structure of porous lattice, and therefore, pore size, shape, and density. However, preparing a contamination-free specimen for AC-HRTEM is challenging. Also, the electron beam can affect sample integrity when the energy transferred is higher than the knockout energy of carbon atoms in the basal plane (20−22 eV)[49] or at the nanopore edge (14 eV).[28] These issues can be avoided to some extent by working at an acceleration voltage of 80 kV or below. While it is not possible to prevent the rearrangement of edge atoms because such events take place with a small energy barriers, imaging at a low acceleration voltage (30 kV)[50] is promising to minimize such events.

Over the past three years, we have developed several specimen preparation strategies to minimize surface contamination, to clean a contaminated lattice, and to perform pore formation experiments directly on the TEM grid. These advancements facilitated the high-throughput analysis of graphene nanopores[51] and helped illucidate etching of graphene by O_3[18,20] and CO_2.[36] A good specimen preparation technique should allow the formation of suspended graphene without any residual contamination from the graphene transfer step. This is crucial for nanoporous graphene samples because contaminants interact more strongly with nanopores compared to the basal plane. Recently, we developed a polymer-free transfer approach that reinforces nanoporous graphene with a premade lacey carbon film with 20−1000 nm openings to produce samples with high coverage and robust enough to withstand further cleaning steps (Figure 8A−D).[51] We also demonstrated that a high-temperature treatment (900 °C) in the presence of activated carbon and using overpressure of H_2 (to avoid an O_2 leak) can remove surface contamination from nanoporous graphene samples without generating new nanopores.[51] An alternative technique to circumvent the contamination issue is to first transfer pristine graphene to a TEM grid, and then subsequently produce the nanopores on the suspended graphene. To achieve this, we adapted the paraffin transfer method developed by Leong et al.[52] to transfer pristine graphene to a holey silicon nitride grid (Figure 8E).[36] This

https://doi.org/10.1021/accountsmr.2c00143
Acc. Mater. Res. 2022, 3, 1073−1087

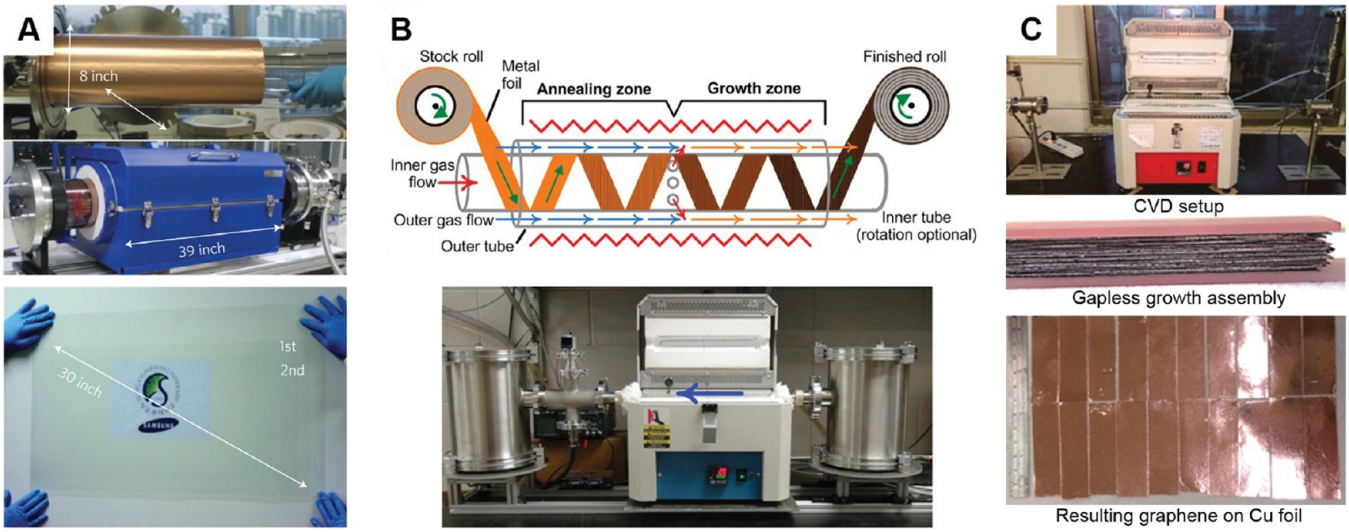

Figure 10. Scale-up of graphene synthesis. (A) Photograph of an 8 in. diameter CVD reactor for large area graphene. Reprinted with permission from ref 8. Copyright 2010 Springer Nature. (B) Schematic and photograph of the roll-to-roll synthesis of graphene film. Reprinted with permission from ref 56. Copyright 2015 The Authors. (C) Photograph of the high-throughput graphene synthesis in stacks. Reprinted with permission from ref 57. Copyright 2016 American Chemical Society.

allowed the study of the CO_2 nanopore etching kinetics by imaging the nanopores before and after an etching step (Figure 8F,G). While it is crucial to develop sample preparation techniques that allow imaging of a large volume of nanopores per sample, it is equally important to develop computational methods capable of efficiently analyzing the increasingly large volume of data. Recently, in this direction, we introduced an advanced image analysis to investigate the grain orientation in nanocrystalline nanoporous graphene samples by calculating the local FFT around each pixel of the HRTEM and using these data to produce an orientation map (Figure 8H−I).[42]

While the advances mentioned above allow characterization of porous graphene lattice, it is currently extremely challenging to resolve functional groups around the nanopores, which tend to gasify during sample preparation and imaging. Ongoing developments in (i) atomic resolution using low electron accelerating voltages,[50] (ii) high-speed imaging by coupling ultrafast isolated electron pulses[53] with direct counting electron detectors,[54] (iii) in situ cleaning protocols, and (iv) scanning atomic electron tomography, will open venues for studying the dynamics of structural changes and the three-dimensional position of atoms and functional groups at the edge of graphene nanopores.

Scanning tunneling microscopy (STM) is emerging as a highly complementary characterization tool for nanoporous graphitic lattice. STM can investigate the surface of nanoporous lattice without modifying the sample including functional groups because of a nondestructive interaction with the sample.[55] As a result, STM facilitates an understanding of pore geometry (PSD, density, functional group surrounding the pores, etc.) by the topography image. Additionally, under low-temperature imaging conditions, one can also probe the nature of functional groups by scanning tunneling spectroscopy. We have used low-temperature STM (LTSTM) operating at 4 K to unravel the mechanistic insights from O_3-based etching of the graphene lattice.[34] We could analyze the density and distribution of epoxy clusters and vacancy defects (Figure 8K−M) and could observe various stages of evolution of clusters into vacancy defects (Figure 8N−P).[34] Advances in sample preparation and improved availability of STM could position it as an extremely popular technique for analyzing the N-SLG lattice.

■ SCALE-UP POTENTIAL

The high performance of N-SLG membrane makes their scale-up a compelling task. N-SLG membranes have come a long way from the first proof-of-principle on micrometer-sized graphene in the year 2008 (Figure 9A).[5] Millimeter-scale and centimeter-scale gas-sieving N-SLG membranes were reported in 2018 and 2021, respectively (Figure 9B−D). Still, several challenges remain in improving the scalability of graphene membranes. Most important of these are a scalable synthesis of N-SLG, transfer on a porous support, and a design of a high-packing-density module. The key technological barrier is the high cost of catalytic metal foil, complex pore generation techniques, and the complex graphene transfer protocol onto a porous support.

CVD is routinely used for synthesizing high-quality SLG (Figure 10).[8,37,56,57] It is an established process and is widely used in the semiconductor industry. Being a vapor-phase technique, obtaining uniform films in a scaled-up reactor is feasible. Efficient packing of copper foils while ensuring a rapid external mass transfer of carbon precursors to Cu, can be used to synthesize large-area graphene, O(100−1000 m^2), in a single batch in a single day inside an industrial CVD reactor (typical diameter of 1 m, length of 1−2 m).

Our group has shown that the cost of copper foil can be reduced by optimizing the surface smoothness of low-cost foils by thermal annealing. Further reduction in the cost of foil can be achieved by developing methods allowing reuse of the foil. Among the pore generation technique, O_3 and O_2 treatments can be adapted to generate pores in a scalable manner. For example, they can be introduced directly inside the CVD reactor after the synthesis of graphene to generate porosity.

The largest hurdle in the scale-up of N-SLG membranes is the transfer of graphene on porous support without inducing cracks and tears. The concept of a gas-permeable mechanical reinforcing layer that can be left permanently on graphene is an

https://doi.org/10.1021/accountsmr.2c00143
Acc. Mater. Res. 2022, 3, 1073−1087

effective strategy for avoiding cracks and tears. The desirable characteristics of the reinforcing materials are strong adhesion to graphene, high intrinsic gas permeance, and robust thermal and chemical stability. We first demonstrated this concept by forming the NPC film on graphene by the pyrolysis of a block copolymer templated turanose (Figure 9B).[14] The NPC film has a perforated lamellar (PL) nanostructure where gas transport takes place in the Knudsen regime via an interlamellar spacing of ∼2 nm.[15] The film terminates with a pore opening of ∼20 nm, over which a graphene layer is suspended. Submicron-thick NPC films have a negligible gas transport resistance (H_2 permeance up to 1 million GPU) because of a rapid transport of gas through the PL nanostructure of NPC. The NPC film binds strongly to graphene, and as a result, graphene membranes with a total area of 1 mm^2 could be prepared on a laser-drilled metal foil support that could be subsequently pressurized to several bars. We extended this approach by further improving the strength of the mechanical reinforcing layer by adding a layer of multiwalled carbon nanotubes (MWNTs) on top of the NPC film (Figure 9C).[16] As a result, centimeter-scale membranes could be prepared on low-cost woven stainless-steel support. Apart from the porous carbon film, an alternative for the mechanical reinforcement layer is gas-permeable dense polymeric films. Highly permeable nanoporous polymeric films that interact well with graphene can allow crack-free transfer of graphene to a porous substrate (Figure 9D).[20,47] This method has the advantage that not only does the polymeric film act as a support but it also acts as a defect sealing film blocking the direct gas-phase transport, and in some cases, can enhance adsorption selectivity. We are now extending this strategy to develop meter-scale membranes under an industry-sponsored pilot plant project for postcombustion capture targeting a capture rate of 10 kg CO_2 per day.[58]

PERSPECTIVE

Membranes with an atom-thick selective layer, such as N-SLG, hold great promise for gas separation because one can avail a large permselective flux, reducing the needed membrane area to reduce the process footprint and capital cost. However, currently, there are several fundamental and engineering challenges in implementing these membranes on a large scale.

The key scientific challenges relate to the synthesis of N-SLG with a high density of pores while maintaining a narrow PSD. For the top-down etching technique, developing a decoupled pore nucleation and pore expansion technique would allow independent control of density and PSD. This can be achieved by generating pore precursors (epoxy clusters) while avoiding gasification events. For the bottom-up direct crystallization route, improved control of grain growth down to the nanometer scale will help tune the size of the grain-boundary defects. This can be achieved by improving the mechanistic understanding of grain growth and subsequently optimizing control handles such as carbon precursor concentration and growth temperature profile. Further control of selectivity can be obtained by postsynthetic modification such as polymer masking or pore functionalization. Here, an extremely desirable direction is to carry out atomic-scale functionalization at the nanopore edge such that the diffusivity across the membrane is not compromised.

As sample preparation and imaging techniques advance, the need for high-throughput computational strategies to identify and analyze a high number of graphene nanopores will be needed to build a better understanding of the structure−property relationship. Currently, the analysis requires a great degree of human intervention to achieve trustworthy results. Further advancements to automatically identify nanopores and to analyze their structure and the neighboring lattice orientation are needed.

From the scale-up point of view, it is important to note that the "quality" of graphene plays a very important role in achieving high-performance membranes. High-quality graphene in this context is single-layer graphene films with a low I_D/I_G ratio (ideally less than 0.05) before any intentional etching step. They should be devoid of any particulate contamination (especially larger than 100 nm), which typically arises when CVD synthesis is carried out in quartz tube reactors. These conditions can be met in a large area CVD reactor by bringing design elements that ensure a good temperature uniformity while avoiding contaminations from the reactor wall.

To advance the technology readiness level of graphene membranes for gas separation, studying separation performance using a realistic gas mixture, e.g., flue gas for postcombustion capture, under relevant operation conditions (temperature, pressure) is needed. Luckily, graphene nanopores are chemically and thermally robust. Proof-of-concept studies have reported attractive separation performances under simulated flue gas conditions (humid feed,[46] elevated temperature,[20,42,46] variable feed pressure[14,16]).

In a recent perspective of membrane separation technology by Beuscher, Kappert, and Wijmans, the need for more holistic research encompassing not only material development but also module and process research was pointed out.[59] Therefore, the fabrication of N-SLG membranes on low-cost supports that can be assembled in a module with a high-packing-density-mimicking spiral wound module (300−1000 m^2/m^3) is needed. Developing roll-to-roll transfer techniques for graphene onto low-cost supports, while at the same time peeling off catalytic substrate for reuse, will be transformative for the field.

AUTHOR INFORMATION

Corresponding Author

Kumar Varoon Agrawal − *Laboratory of Advanced Separations, École Polytechnique Fédérale de Lausanne, Sion 1950, Switzerland;* orcid.org/0000-0002-5170-6412; Email: kumar.agrawal@epfl.ch

Authors

Luis Francisco Villalobos − *Laboratory of Advanced Separations, École Polytechnique Fédérale de Lausanne, Sion 1950, Switzerland;* orcid.org/0000-0002-0745-4246

Deepu J. Babu − *Laboratory of Advanced Separations, École Polytechnique Fédérale de Lausanne, Sion 1950, Switzerland; Department of Materials Science and Metallurgical Engineering, Indian Institute of Technology, Hyderabad, Telangana 502 284, India;* orcid.org/0000-0003-2593-4013

Kuang-Jung Hsu − *Laboratory of Advanced Separations, École Polytechnique Fédérale de Lausanne, Sion 1950, Switzerland*

Cédric Van Goethem − *Laboratory of Advanced Separations, École Polytechnique Fédérale de Lausanne, Sion 1950, Switzerland*

https://doi.org/10.1021/accountsmr.2c00143
Acc. Mater. Res. 2022, 3, 1073−1087

Complete contact information is available at:
https://pubs.acs.org/10.1021/accountsmr.2c00143

Author Contributions

#L.F.V., D.J.B., K.-J.H., and G.V.G. contributed equally to this work.

Notes

The authors declare no competing financial interest.

Biographies

Luis Francisco Villalobos received his Ph.D. in chemical engineering at King Abdullah University of Science and Technology in 2017. He worked as a postdoctoral researcher at EPFL, before joining Yale University as SNSF postdoctoral fellow. His research interests focus on understanding the mechanisms behind the selective transport of molecules and on developing novel membrane technologies for the sustainable production of critical materials and energy.

Deepu J. Babu received his Ph.D. from TU Darmstadt, Germany, in 2016. He worked as a postdoctoral researcher at EPFL before joining IIT Hyderabad as an assistant professor. His research interests are in the field of porous materials and understanding the nucleation and growth of low-dimensional materials.

Kuang-Jung Hsu received his Master degree in chemical engineering at National Taiwan university in 2018 and is now a Ph.D. candidate at EPFL. His research interests are engineering and functionalization chemistry on Å-scale nanopores on single-layer graphene for gas separation. He is also interested in developing the atomic thin membranes for the postcombustion carbon capture.

Cédric Van Goethem received his Ph.D. in bioscience engineering with Prof. Ivo Vankelecom at KU Leuven, Belgium, in 2018. He continued working at KU Leuven as a postdoctoral researcher before joining EPFL in 2020. His research interests focus on the development of membrane materials for sustainable molecular separations with a focus on the bottom-up synthesis of nanoporous graphene.

Kumar Varoon Agrawal is an assistant professor and GAZNAT chair of Advanced Separation at EPFL. His research interests focus on material chemistry and engineering at Å-scale for the development of energy-efficient inorganic and hybrid membranes for molecular separation. He has keen interest in the fundamental aspects of nanoporous 2D materials as well as in the scale-up of high-performance membranes based on these materials.

■ ACKNOWLEDGMENTS

We acknowledge the host institution EPFL for support. We thank European Research Council Starting Grant (805437-UltimateMembranes), Shell, and GAZNAT for funding the work. L.F.V. thanks the Swiss National Science Foundation for the Postdoc.Mobility Fellowship (P400P2_199330).

■ REFERENCES

(1) Freeman, B. D. Basis of Permeability/Selectivity Tradeoff Relations in Polymeric Gas Separation Membranes. *Macromolecules* **1999**, *32* (2), 375−380.
(2) Robeson, L. M. The Upper Bound Revisited. *J. Membr. Sci.* **2008**, *320* (1), 390−400.
(3) Wang, L.; Boutilier, M. S. H.; Kidambi, P. R.; Jang, D.; Hadjiconstantinou, N. G.; Karnik, R. Fundamental Transport Mechanisms, Fabrication and Potential Applications of Nanoporous Atomically Thin Membranes. *Nat. Nanotechnol.* **2017**, *12* (6), 509−522.
(4) Kidambi, P. R.; Chaturvedi, P.; Moehring, N. K. Subatomic Species Transport through Atomically Thin Membranes: Present and Future Applications. *Science* **2021**, *374* (6568), eabd7687.
(5) Bunch, J. S.; Verbridge, S. S.; Alden, J. S.; Van Der Zande, A. M.; Parpia, J. M.; Craighead, H. G.; McEuen, P. L. Impermeable Atomic Membranes from Graphene Sheets. *Nano Lett.* **2008**, *8* (8), 2458−2462.
(6) Cohen-Tanugi, D.; Grossman, J. C. Mechanical Strength of Nanoporous Graphene as a Desalination Membrane. *Nano Lett.* **2014**, *14* (11), 6171−6178.
(7) Wang, L.; Williams, C. M.; Boutilier, M. S. H.; Kidambi, P. R.; Karnik, R. Single-Layer Graphene Membranes Withstand Ultrahigh Applied Pressure. *Nano Lett.* **2017**, *17* (5), 3081−3088.
(8) Bae, S.; Kim, H.; Lee, Y.; Xu, X.; Park, J.-S.; Zheng, Y.; Balakrishnan, J.; Lei, T.; Ri Kim, H.; Song, Y. Il; Kim, Y.-J.; Kim, K. S.; Özyilmaz, B.; Ahn, J.-H.; Hong, B. H.; Iijima, S. Roll-to-Roll Production of 30-Inch Graphene Films for Transparent Electrodes. *Nat. Nanotechnol.* **2010**, *5* (8), 574−578.
(9) Kobayashi, T.; Bando, M.; Kimura, N.; Shimizu, K.; Kadono, K.; Umezu, N.; Miyahara, K.; Hayazaki, S.; Nagai, S.; Mizuguchi, Y. Production of a 100-m-Long High-Quality Graphene Transparent Conductive Film by Roll-to-Roll Chemical Vapor Deposition and Transfer Process. *Appl. Phys. Lett.* **2013**, *102* (2), 023112.
(10) Jiang, D.; Cooper, V. R.; Dai, S. Porous Graphene as the Ultimate Membrane for Gas Separation. *Nano Lett.* **2009**, *9* (12), 4019−4024.
(11) Schrier, J. Carbon Dioxide Separation with a Two-Dimensional Polymer Membrane. *ACS Appl. Mater. Interfaces* **2012**, *4* (7), 3745−3752.
(12) Liu, H.; Dai, S.; Jiang, D. Insights into CO2/N2 Separation through Nanoporous Graphene from Molecular Dynamics. *Nanoscale* **2013**, *5* (20), 9984.
(13) Koenig, S. P.; Wang, L.; Pellegrino, J.; Bunch, J. S. Selective Molecular Sieving through Porous Graphene. *Nat. Nanotechnol.* **2012**, *7* (11), 728−732.
(14) Huang, S.; Dakhchoune, M.; Luo, W.; Oveisi, E.; He, G.; Rezaei, M.; Zhao, J.; Alexander, D. T. L.; Züttel, A.; Strano, M. S.; Agrawal, K. V. Single-Layer Graphene Membranes by Crack-Free Transfer for Gas Mixture Separation. *Nat. Commun.* **2018**, *9* (1), 2632.
(15) Dakhchoune, M.; Duan, X.; Villalobos, L. F.; Hsu, K.-J.; Zhao, J.; Micari, M.; Agrawal, K. V. Rapid Gas Transport from Block-Copolymer Templated Nanoporous Carbon Films. *Ind. Eng. Chem. Res.* **2021**, *60* (44), 16100−16108.
(16) Lee, W. C.; Bondaz, L.; Huang, S.; He, G.; Dakhchoune, M.; Agrawal, K. V. Centimeter-Scale Gas-Sieving Nanoporous Single-Layer Graphene Membrane. *J. Membr. Sci.* **2021**, *618*, No. 118745.
(17) Zhao, J.; He, G.; Huang, S.; Villalobos, L. F.; Dakhchoune, M.; Bassas, H.; Agrawal, K. V. Etching Gas-Sieving Nanopores in Single-Layer Graphene with an Angstrom Precision for High-Performance Gas Mixture Separation. *Sci. Adv.* **2019**, *5* (1), No. eaav1851.
(18) Hsu, K. J.; Villalobos, L. F.; Huang, S.; Chi, H. Y.; Dakhchoune, M.; Lee, W. C.; He, G.; Mensi, M.; Agrawal, K. V. Multipulsed Millisecond Ozone Gasification for Predictable Tuning of Nucleation and Nucleation-Decoupled Nanopore Expansion in Graphene for Carbon Capture. *ACS Nano* **2021**, *15* (8), 13230−13239.
(19) Huang, S.; Li, S.; Hsu, K.-J.; Villalobos, L. F.; Agrawal, K. V. Systematic Design of Millisecond Gasification Reactor for the Incorporation of Gas-Sieving Nanopores in Single-Layer Graphene. *J. Membr. Sci.* **2021**, *637*, No. 119628.
(20) Huang, S.; Li, S.; Villalobos, L. F.; Dakhchoune, M.; Micari, M.; Babu, D. J.; Vahdat, M. T.; Mensi, M.; Oveisi, E.; Agrawal, K. V. Millisecond Lattice Gasification for High-Density CO 2 - and O 2 -Sieving Nanopores in Single-Layer Graphene. *Sci. Adv.* **2021**, *7* (9), No. eabf0116.
(21) Garaj, S.; Hubbard, W.; Reina, A.; Kong, J.; Branton, D.; Golovchenko, J. A. Graphene as a Subnanometre Trans-Electrode Membrane. *Nature* **2010**, *467* (7312), 190−193.

(22) Celebi, K.; Buchheim, J.; Wyss, R. M.; Droudian, A.; Gasser, P.; Shorubalko, I.; Kye, J.-I.; Lee, C.; Park, H. G. Ultimate Permeation Across Atomically Thin Porous Graphene. *Science* **2014**, *344* (6181), 289−292.
(23) Yamada, Y.; Murota, K.; Fujita, R.; Kim, J.; Watanabe, A.; Nakamura, M.; Sato, S.; Hata, K.; Ercius, P.; Ciston, J.; Song, C. Y.; Kim, K.; Regan, W.; Gannett, W.; Zettl, A. Subnanometer Vacancy Defects Introduced on Graphene by Oxygen Gas. *J. Am. Chem. Soc.* **2014**, *136* (6), 2232−2235.
(24) Surwade, S. P.; Smirnov, S. N.; Vlassiouk, I. V.; Unocic, R. R.; Veith, G. M.; Dai, S.; Mahurin, S. M. Water Desalination Using Nanoporous Single-Layer Graphene. *Nat. Nanotechnol.* **2015**, *10* (5), 459−464.
(25) Yang, Y.; Yang, X.; Liang, L.; Gao, Y.; Cheng, H.; Li, X.; Zou, M.; Ma, R.; Yuan, Q.; Duan, X. Large-Area Graphene-Nanomesh/Carbon-Nanotube Hybrid Membranes for Ionic and Molecular Nanofiltration. *Science* **2019**, *364* (6445), 1057−1062.
(26) Agrawal, K. V.; Benck, J. D.; Yuan, Z.; Misra, R. P.; Govind Rajan, A.; Eatmon, Y.; Kale, S.; Chu, X. S.; Li, D. O.; Gong, C.; Warner, J.; Wang, Q. H.; Blankschtein, D.; Strano, M. S. Fabrication, Pressure Testing, and Nanopore Formation of Single-Layer Graphene Membranes. *J. Phys. Chem. C* **2017**, *121* (26), 14312−14321.
(27) Buchheim, J.; Wyss, R. M.; Shorubalko, I.; Park, H. G. Understanding the Interaction between Energetic Ions and Free-standing Graphene towards Practical 2D Perforation. *Nanoscale* **2016**, *8* (15), 8345−8354.
(28) Russo, C. J.; Golovchenko, J. A. Atom-by-Atom Nucleation and Growth of Graphene Nanopores. *Proc. Natl. Acad. Sci. U. S. A.* **2012**, *109* (16), 5953−5957.
(29) Jang, D.; Idrobo, J. C.; Laoui, T.; Karnik, R. Water and Solute Transport Governed by Tunable Pore Size Distributions in Nanoporous Graphene Membranes. *ACS Nano* **2017**, *11* (10), 10042−10052.
(30) Li, J.-L.; Kudin, K. N.; McAllister, M. J.; Prud'homme, R. K.; Aksay, I. A.; Car, R. Oxygen-Driven Unzipping of Graphitic Materials. *Phys. Rev. Lett.* **2006**, *96* (17), No. 176101.
(31) Sun, T.; Fabris, S. Mechanisms for Oxidative Unzipping and Cutting of Graphene. *Nano Lett.* **2012**, *12* (1), 17−21.
(32) Lee, G.; Lee, B.; Kim, J.; Cho, K. Ozone Adsorption on Graphene: Ab Initio Study and Experimental Validation. *J. Phys. Chem. C* **2009**, *113* (32), 14225−14229.
(33) Larciprete, R.; Fabris, S.; Sun, T.; Lacovig, P.; Baraldi, A.; Lizzit, S. Dual Path Mechanism in the Thermal Reduction of Graphene Oxide. *J. Am. Chem. Soc.* **2011**, *133* (43), 17315−17321.
(34) Li, S.; Vahdat, M. T.; Huang, S.; Hsu, K.-J.; Rezaei, M.; Mensi, M.; Marzari, N.; Agrawal, K. V. Structure Evolution of Graphitic Surface upon Oxidation: Insights by Scanning Tunneling Microscopy. *JACS Au* **2022**, *2* (3), 723−730.
(35) Li, Z.; Zhang, W.; Luo, Y.; Yang, J.; Hou, J. G. How Graphene Is Cut upon Oxidation? *J. Am. Chem. Soc.* **2009**, *131* (18), 6320−6321.
(36) Rezaei, M.; Villalobos, L. F.; Hsu, K.-J.; Agrawal, K. V. Demonstrating and Unraveling a Controlled Nanometer-Scale Expansion of the Vacancy Defects in Graphene by CO 2. *Angew. Chem.* **2022**, *61* (18), No. 202200321.
(37) Kidambi, P. R.; Nguyen, G. D.; Zhang, S.; Chen, Q.; Kong, J.; Warner, J.; Li, A.-P.; Karnik, R. Facile Fabrication of Large-Area Atomically Thin Membranes by Direct Synthesis of Graphene with Nanoscale Porosity. *Adv. Mater.* **2018**, *30* (49), No. 1804977.
(38) Khan, M. H.; Moradi, M.; Dakhchoune, M.; Rezaei, M.; Huang, S.; Zhao, J.; Agrawal, K. V. Hydrogen Sieving from Intrinsic Defects of Benzene-Derived Single-Layer Graphene. *Carbon* **2019**, *153*, 458−466.
(39) Rezaei, M.; Li, S.; Huang, S.; Agrawal, K. V. Hydrogen-Sieving Single-Layer Graphene Membranes Obtained by Crystallographic and Morphological Optimization of Catalytic Copper Foil. *J. Membr. Sci.* **2020**, *612* (July), No. 118406.
(40) Bhaviripudi, S.; Jia, X.; Dresselhaus, M. S.; Kong, J. Role of Kinetic Factors in Chemical Vapor Deposition Synthesis of Uniform Large Area Graphene Using Copper Catalyst. *Nano Lett.* **2010**, *10* (10), 4128−4133.
(41) Liu, M.; Zhang, Y.; Chen, Y.; Gao, Y.; Gao, T.; Ma, D.; Ji, Q.; Zhang, Y.; Li, C.; Liu, Z. Thinning Segregated Graphene Layers on High Carbon Solubility Substrates of Rhodium Foils by Tuning the Quenching Process. *ACS Nano* **2012**, *6* (12), 10581−10589.
(42) Villalobos, L. F.; Van Goethem, C.; Hsu, K.-J.; Li, S.; Moradi, M.; Zhao, K.; Dakhchoune, M.; Huang, S.; Shen, Y.; Oveisi, E.; Boureau, V.; Agrawal, K. V. Bottom-up Synthesis of Graphene Films Hosting Atom-Thick Molecular-Sieving Apertures. *Proc. Natl. Acad. Sci. U. S. A.* **2021**, *118* (37), No. e2022201118.
(43) Sun, C.; Zhu, S.; Liu, M.; Shen, S.; Bai, B. Selective Molecular Sieving through a Large Graphene Nanopore with Surface Charges. *J. Phys. Chem. Lett.* **2019**, *10* (22), 7188−7194.
(44) Tian, Z.; Mahurin, S. M.; Dai, S.; Jiang, D. Ion-Gated Gas Separation through Porous Graphene. *Nano Lett.* **2017**, *17* (3), 1802−1807.
(45) Guo, W.; Mahurin, S. M.; Unocic, R. R.; Luo, H.; Dai, S. Broadening the Gas Separation Utility of Monolayer Nanoporous Graphene Membranes by an Ionic Liquid Gating. *Nano Lett.* **2020**, *20* (11), 7995−8000.
(46) He, G.; Huang, S.; Villalobos, L. F.; Zhao, J.; Mensi, M.; Oveisi, E.; Rezaei, M.; Agrawal, K. V. High-Permeance Polymer-Functionalized Single-Layer Graphene Membranes That Surpass the Postcombustion Carbon Capture Target. *Energy Environ. Sci.* **2019**, *12* (11), 3305−3312.
(47) He, G.; Huang, S.; Villalobos, L. F.; Vahdat, M. T.; Guiver, M. D.; Zhao, J.; Lee, W.; Mensi, M.; Agrawal, K. V. Synergistic CO 2 -Sieving from Polymer with Intrinsic Microporosity Masking Nanoporous Single-Layer Graphene. *Adv. Funct. Mater.* **2020**, *30* (39), No. 2003979.
(48) He, G.; Huang, S.; Villalobos, L. F.; Vahdat, M. T.; Guiver, M. D.; Zhao, J.; Lee, W. C.; Mensi, M.; Agrawal, K. V. Synergistic CO2-Sieving from Polymer with Intrinsic Microporosity Masking Nanoporous Single-Layer Graphene. *Adv. Funct. Mater.* **2020**, *30* (39), No. 2003979.
(49) Meyer, J. C.; Eder, F.; Kurasch, S.; Skakalova, V.; Kotakoski, J.; Park, H. J.; Roth, S.; Chuvilin, A.; Eyhusen, S.; Benner, G.; Krasheninnikov, A. V.; Kaiser, U. Accurate Measurement of Electron Beam Induced Displacement Cross Sections for Single-Layer Graphene. *Phys. Rev. Lett.* **2012**, *108* (19), 1−6.
(50) Börrnert, F.; Kaiser, U. Chromatic- and Geometric-Aberration-Corrected TEM Imaging at 80 KV and 20 KV. *Phys. Rev. A* **2018**, *98* (2), No. 023861.
(51) Villalobos, L. F.; Huang, S.; Dakhchoune, M.; He, G.; Lee, W.-C.; Agrawal, K. V. Polybenzimidazole Copolymer Derived Lacey Carbon Film for Graphene Transfer and Contamination Removal Strategies for Imaging Graphene Nanopores. *Carbon* **2021**, *173*, 980−988.
(52) Leong, W. S.; Wang, H.; Yeo, J.; Martin-Martinez, F. J.; Zubair, A.; Shen, P. C.; Mao, Y.; Palacios, T.; Buehler, M. J.; Hong, J. Y.; Kong, J. Paraffin-Enabled Graphene Transfer. *Nat. Commun.* **2019**, *10* (1), 1−8.
(53) Hassan, M. T.; Baskin, J. S.; Liao, B.; Zewail, A. H. High-Resolution Electron Microscopy for Imaging Ultrafast Electron Dynamics. *Nat. Photonics* **2017**, *11* (7), 425−430.
(54) Mir, J. A.; Clough, R.; MacInnes, R.; Gough, C.; Plackett, R.; Shipsey, I.; Sawada, H.; MacLaren, I.; Ballabriga, R.; Maneuski, D.; O'Shea, V.; McGrouther, D.; Kirkland, A. I. Characterisation of the Medipix3 Detector for 60 and 80 KeV Electrons. *Ultramicroscopy* **2017**, *182*, 44−53.
(55) Giessibl, F. J. Atomic Resolution on Si(111)-(7 × 7) by Noncontact Atomic Force Microscopy with a Force Sensor Based on a Quartz Tuning Fork. *Appl. Phys. Lett.* **2000**, *76* (11), 1470−1472.
(56) Polsen, E. S.; McNerny, D. Q.; Viswanath, B.; Pattinson, S. W.; John Hart, A. High-Speed Roll-to-Roll Manufacturing of Graphene Using a Concentric Tube CVD Reactor. *Sci. Rep.* **2015**, *5*, 1−12.

https://doi.org/10.1021/accountsmr.2c00143
Acc. Mater. Res. 2022, 3, 1073−1087

(57) Hsieh, Y. P.; Shih, C. H.; Chiu, Y. J.; Hofmann, M. High-Throughput Graphene Synthesis in Gapless Stacks. *Chem. Mater.* **2016**, *28* (1), 40−43.
(58) Agrawal, K. V.; Bautz, R. *Capture Du Carbone Par Membranes En Graphène à Nanopores*; Aqua Gas, 2022; 46−53.
(59) Beuscher, U.; Kappert, E. J.; Wijmans, J. G. Membrane Research beyond Materials Science. *J. Membr. Sci.* **2022**, *643*, No. 119902.

https://doi.org/10.1021/accountsmr.2c00143
Acc. Mater. Res. 2022, 3, 1073−1087